

Variable-length Convolutional Coding for Short Blocklengths with Decision Feedback

Adam R. Williamson, *Student Member, IEEE*, Tsung-Yi Chen, *Member, IEEE*,
and Richard D. Wesel, *Senior Member, IEEE*

Abstract

This paper presents a variable-length decision-feedback scheme that uses tail-biting convolutional codes and the tail-biting Reliability-Output Viterbi Algorithm (ROVA). Comparing with recent results in finite-blocklength information theory, simulation results for both the BSC and the AWGN channel show that the decision-feedback scheme using ROVA can surpass the random-coding lower bound on throughput for feedback codes at average blocklengths less than 100 symbols. This paper explores ROVA-based decision feedback both with decoding after every symbol and with decoding limited to a small number of increments. The performance of the reliability-based stopping rule with the ROVA is compared to retransmission decisions based on CRCs. For short blocklengths where the latency overhead of the CRC bits is severe, the ROVA-based approach delivers superior rates.

Index Terms

Feedback communication, Error correction and detection coding, Convolutional codes, CRCs

A. R. Williamson and R. D. Wesel are with the EE Dept., UCLA, Los Angeles, CA 90095 USA (adam.williamson.us@ieee.org; wesel@ee.ucla.edu). T.-Y. Chen is with the Dept. of EECS, Northwestern University, Evanston, IL 60208 USA (tsungyi.chen@northwestern.edu). Portions of this work were presented at the 2013 Int. Symp. on Inf. Theory (ISIT) in Istanbul, Turkey. This material is based upon work supported by the National Science Foundation under Grant Number 1162501. Any opinions, findings, and conclusions or recommendations expressed in this material are those of the author(s) and do not necessarily reflect the views of the National Science Foundation.

I. INTRODUCTION

A. Overview and Related Literature

Despite Shannon’s 1956 result [1] that noiseless feedback does not increase the asymptotic capacity of point-to-point, memoryless channels, feedback has other benefits for these channels that have made it a staple in modern communication systems. For example, feedback can simplify encoding and decoding operations and has been incorporated into incremental redundancy (IR) schemes proposed at least as early as 1974 [2]. Hagenauer’s introduction of rate-compatible punctured convolutional (RCPC) codes allows the same encoder to be used under varying channel conditions with feedback determining when to send additional coded bits [3]. Additionally, feedback can significantly improve the error exponent, which governs the error probability as a function of blocklength (see, e.g., [4]).

Perhaps the most important benefit of feedback is its ability to reduce the average blocklength required to approach capacity. Polyanskiy, Poor and Verdú [5] quantified the backoff from capacity at finite blocklengths without feedback, demonstrating that short blocklengths impose a severe penalty on the maximum achievable rate. Even when the best fixed-length block code is paired with an Automatic Repeat reQuest (ARQ) strategy, the maximum rate is slow to converge to the asymptotic (Shannon) capacity. However, when variable-length coding is used on channels with noiseless feedback, the maximum rate improves dramatically for short (average) blocklengths [6].

Practical considerations for variable-length codes motivated Chen et al. [7], [8] to study the effects of periodic decoding (i.e., only decoding and sending feedback after every $I > 1$ symbols). The analysis in [7] and [8] used IR in the context of finite-length-codes, showing that a length- N code can be used in a variable-length transmission scheme and provide the same performance as an infinite-length code (as in [6]), up to second order terms. The importance of these results is that “good” finite-length codes can still achieve rates approaching capacity

at short blocklengths. Contemporaneous with [5] and [6], Chen et al. [9], [10] showed that the relatively simple decoding of short-blocklength convolutional codes in an IR setting could match the throughput delivered by long-blocklength turbo codes. This led to the subsequent work in [7] and [8], which made connections between the theory and practical codes. IR and hybrid ARQ have also been discussed elsewhere in the recent communication literature (e.g., [11]–[13]), but those papers are not focused on characterizing the maximum rate at short average blocklengths.

B. Contributions

In this paper, we investigate the performance of variable-length feedback (VLF) codes with average blocklengths less than 300 symbols. In the VLF coding framework of Polyanskiy et al. [6], the receiver determines when to stop transmission and informs the transmitter via noiseless feedback. This is different from the variable-length feedback codes *with termination* (VLFT) introduced in [6] and explored in [7], [8], which use a special noiseless termination symbol on the forward channel to indicate when to stop. Here we evaluate the short-blocklength performance of VLF codes with *decision* feedback, in which feedback is only used to inform the transmitter when to stop. This is in contrast to *information*-feedback VLF codes, which allow the transmitter to adapt its transmission based on information about the previously received symbols. See, e.g., [14] for an investigation of information feedback at short blocklengths.

There is a large gap between the lower and upper bounds in [6] on achievable rate at short blocklengths for VLF codes. This paper demonstrates explicit decision-feedback coding schemes that surpass the random-coding lower bound in [6]. These schemes use convolutional codes due to their excellent performance at short blocklengths. Numerical examples are given for the binary symmetric channel (BSC) and binary-input additive white Gaussian noise (BI-AWGN) channel.

The decision-feedback scheme in Williamson et al. [15] uses Raghavan and Baum’s Reliability-Output Viterbi Algorithm (ROVA) [16] for terminated convolutional codes to compute the posterior probability of the decoded word and stops transmission when that word is sufficiently

likely. This is similar to the reliability-based retransmission scheme in Fricke et al. [13], except that Fricke et al. is not focused on evaluating the short-blocklength performance. While the reliability-based retransmission scheme in [15] delivers high rates at relatively short blocklengths, the termination of the convolutional codes introduces rate loss at the shortest blocklengths.

Tail-biting (TB) convolutional codes, on the other hand, start and end in the same state, though that starting/ending state is unknown at the receiver. In exchange for increased decoding complexity compared to terminated convolutional codes, TB codes do not suffer from rate loss at short blocklengths. However, Raghavan and Baum’s ROVA [16] applies only to terminated convolutional codes. In [17], Williamson et al. introduce a reliability-output decoder for TB convolutional codes, called the TB ROVA. This paper compares a reliability-based retransmission scheme using the TB ROVA with an alternative approach using Cyclic Redundancy Checks (CRCs), called code-based error detection. Both the ROVA and the TB ROVA allow the decoder to request retransmissions without requiring parity bits to be sent for error detection.

When delay constraints or other practical considerations preclude decoding after every symbol, decoding after groups of symbols is required. Selecting the incremental transmission lengths that maximize the throughput is non-trivial, however. Appendix C provides a numerical optimization algorithm for selecting the m optimal blocklengths in a general m -transmission IR scheme. Appendix D particularizes this algorithm to the reliability-based scheme using the TB ROVA.

The new contributions relative to our precursor conference paper [15] are as follows: this paper incorporates the TB ROVA of [17], investigates the performance of “packet” transmissions by introducing a novel blocklength-selection algorithm, compares ROVA-based retransmission to CRC-based retransmission, and extends bounds in [6] to repeat-after- N codes. The remainder of this paper proceeds as follows: Sec. I-C introduces relevant notation. Sec. II reviews the fundamental limits for VLF codes from [6] and presents several extensions of the random-coding lower bound to VLF systems with “packets”. Sec. III evaluates the performance of ROVA-based and CRC-based stopping rules in the decision-feedback setting. Sec. IV concludes the paper.

C. Notation

In general, capital letters denote random variables and lowercase letters denote their realizations (e.g., random variable Y and value y). Superscripts denote vectors unless otherwise noted, as in $y^\ell = (y_1, y_2, \dots, y_\ell)$, while subscripts denote a particular element of a vector: y_i is the i th element of y^ℓ . The expressions involving $\log(\cdot)$ and $\exp\{\cdot\}$ in information-theoretic derivations are valid for any base, but numerical examples use base 2 and present results in units of bits.

II. VLF CODING FRAMEWORK

A. Finite-blocklength Information Theory

For finite-length block codes without feedback, Polyanskiy et al. [5] provide achievability (lower) and converse (upper) bounds on the maximum rate, along with a normal approximation of the information density that can approximate both bounds for moderate blocklengths. In contrast to this tight characterization of the no-feedback case, there is a large gap between the lower and upper bounds for VLF codes at short average blocklengths presented in Polyanskiy et al. [6]. This section reviews the fundamental limits for VLF codes from [6] and provides extensions of the lower bound to repeat-after- N codes, which are similar in principle to the finite-length VLFT codes studied in [7], [8]. This framework will allow us to evaluate the short-blocklength performance of the decision-feedback schemes in Sec. III in terms of these fundamental limits.

We assume there is a noiseless feedback channel. The noisy forward channel is memoryless, has input alphabet \mathcal{X} and has output alphabet \mathcal{Y} . The channel satisfies

$$P(Y_n|X^n, Y^{n-1}) = P(Y_n|X_n) = P(Y_1|X_1) \quad \forall n = 1, 2, \dots \quad (1)$$

A discrete, memoryless channel (DMC) is a special case when \mathcal{X} and \mathcal{Y} are countable.

Definition 1. (From [6]) An (ℓ, M, ϵ) **variable-length feedback (VLF)** code is defined by:

- A message $W \in \mathcal{W} = \{1, \dots, M\}$, assumed to be equiprobable. (The positive integer M is the cardinality of the message set \mathcal{W} .)

- A random variable $U \in \mathcal{U}$ and a probability distribution P_U on the space \mathcal{U} . U represents common randomness that is revealed to both transmitter and receiver before communication begins, which facilitates the use of random-coding arguments in the sequel.
- A sequence of encoder functions $f_n : \mathcal{U} \times \mathcal{W} \times \mathcal{Y}^{n-1} \rightarrow \mathcal{X}, n \geq 1$, which defines the n th channel input:

$$X_n = f_n(U, W, Y^{n-1}). \quad (2)$$

- A sequence of decoder functions $g_n : \mathcal{U} \times \mathcal{Y}^n \rightarrow \mathcal{W}, n \geq 1$, providing an estimate \hat{W}_n of the message W :

$$\hat{W}_n = g_n(U, Y^n). \quad (3)$$

- An integer-valued random variable $\tau \geq 0$, which is a stopping time of the filtration $\mathcal{G}_n = \sigma\{U, Y_1, \dots, Y_n\}$. The stopping time satisfies

$$\mathbb{E}[\tau] \leq \ell. \quad (4)$$

- A final decision computed at time τ , at which the error probability must be less than ϵ ($0 \leq \epsilon \leq 1$):

$$\mathbb{P}[\hat{W}_\tau \neq W] \leq \epsilon. \quad (5)$$

In the definition above, the receiver attempts to decode after each received symbol. Because the final decision is not computed until time $n = \tau$, the estimates \hat{W}_n in (3) for $n < \tau$ may be considered tentative estimates that do not affect the decoding outcome. This differs slightly from [6], which does not require the decoder to compute the tentative estimates $g_n(U, Y^n)$ for $n < \tau$. We include the definition of \hat{W}_n here for consistency with the reliability-based stopping approach in Sec. III. The receiver uses some stopping rule (to be specified in Sec. III) to determine when to stop decoding and informs the transmitter via feedback. This VLF coding framework is illustrated in Fig. 1. Eq. (4) indicates that for an (ℓ, M, ϵ) VLF code, the expected length will be no more than ℓ . The rate R is given as $R = \frac{\log M}{\ell}$.

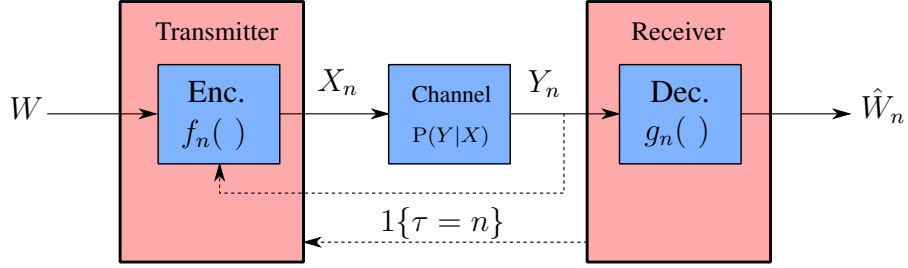


Fig. 1. Illustration of the VLF coding framework, with message W , encoder (Enc.) output X_n at time n , memoryless channel output Y_n , and decoder (Dec.) estimate \hat{W}_n . The feedback link (dashed line) to the encoder is assumed to be noiseless. With decision feedback, the transmitter disregards the received symbols Y_n and only uses feedback to determine whether to stop (i.e., when $\tau = n$).

Polyanskiy et al. [6] define a class of VLF codes called *stop-feedback codes* that satisfy:

$$f_n(U, W, Y^{n-1}) = f_n(U, W). \quad (6)$$

For stop-feedback codes, the encoded symbols are independent of the previously received noisy-channel outputs. The feedback link is used only to inform the transmitter when the receiver has determined that the transmission should terminate. This paradigm was referred to as *decision feedback* in early papers by Chang [18] and by Forney [19], the term which we will use in the sequel, and as a channel used without feedback by Massey [20].

Decision-feedback codes are practically relevant because they require only one bit of feedback for the receiver to communicate its termination decision (i.e., to stop or to request additional symbols). This feedback bit is usually referred to as an ACK (acknowledgment) or NACK (negative acknowledgment). A consequence of the decision-feedback restriction is that the codeword corresponding to message W , $\{X_n(W)\}_{n=1}^{\infty}$, can be generated before any symbols are transmitted over the channel, as the codeword does not depend on the realizations of $\{Y_n\}_{n=1}^{\infty}$.

In contrast, VLF codes for which (6) is not generally true are referred to as information-feedback codes. The most general form of information feedback is for the receiver to send each of its received symbols Y_n to the transmitter. With information feedback, the transmitter may

adapt its transmissions based on this feedback, directing the receiver to the correct codeword. Naghshvar et al. [21], [22] discuss this type of feedback in the context of active sequential hypothesis testing and demonstrate a deterministic, sequential coding scheme for DMCs that achieves the optimal error-exponent.

B. Fundamental Limits for VLF Codes

The VLF converse bounds referenced in this paper come from Polyanskiy et al. [6, Theorem 4] and [6, Theorem 6]. The latter [6, Theorem 6] applies only to channels with finite maximal relative entropy C_1 , but provides a tighter upper bound than [6, Theorem 4].

The following VLF achievability theorems make use of the information density at blocklength n , $i(x^n; y^n)$, defined as

$$i(x^n; y^n) = \log \frac{dP(Y^n = y^n | X^n = x^n)}{dP(Y^n = y^n)}. \quad (7)$$

Theorem 1 (Random-coding lower bound [6, Theorem 3]). *For a scalar $\gamma > 0$, \exists an (ℓ, M, ϵ) VLF code satisfying*

$$\ell \leq E[\tau], \quad (8)$$

$$\epsilon \leq (M - 1)P[\bar{\tau} \leq \tau], \quad (9)$$

where γ is a threshold for the hitting times τ and $\bar{\tau}$:

$$\tau = \inf\{n \geq 0 : i(X^n; Y^n) \geq \gamma\} \quad (10)$$

$$\bar{\tau} = \inf\{n \geq 0 : i(\bar{X}^n; Y^n) \geq \gamma\}, \quad (11)$$

and where \bar{X}^n is distributed identically to X^n , but is independent of (X^n, Y^n) .

Thm. 1 gives an upper bound on average blocklength ℓ and therefore a lower bound on achievable rate for codes with cardinality M and error probability ϵ . However, it is not always straightforward to compute the achievable $(\ell, \frac{\log M}{\ell})$ pairs. In [15, Appendix B], Williamson et al.

provide a method for computing these blocklength-rate pairs, based on numerical evaluation of an infinite sum. For the AWGN channel, each term in the sum requires a 3-dimensional numerical integration. In Appendix A of this paper, we describe a different method of computing the average stopping time $E[\tau]$ in (8) based on Wald's equality [23, Ch. 5]. This technique is computationally simpler and does not suffer from numerical accuracy issues that arise in evaluating an infinite sum. As explained in Appendix A, the new method applies only to channels with bounded information density $i(X_n; Y_n)$ (e.g, the BSC or BI-AWGN channel, but not the AWGN channel with real-valued inputs).

It is straightforward to extend Polyanskiy et al.'s random-coding lower bound [6] to VLF codes derived from repeating length- N mother codes, which we will show in Cor. 1. We begin by defining (ℓ, M, ϵ) repeat-after- N VLF codes, in which the coded symbols for $n > N$ repeat the first N symbols. Let $r \in \{1, \dots, N\}$ be the index within each block of N symbols, i.e., $n = sN + r$ for some $s \in \{0, 1, \dots\}$.

Definition 2. An (ℓ, M, ϵ) repeat-after- N VLF code is defined as in Def. 1, except the following are different:

- A sequence of encoder functions $f_r : \mathcal{U} \times \mathcal{W} \times \mathcal{Y}_{sN+1}^{n-1} \rightarrow \mathcal{X}$, which defines the n th channel input, where $r \in \{1, \dots, N\}$, $n \geq 1$, $s = \lfloor \frac{n-1}{N} \rfloor$:

$$X_n = f_r(U, W, Y_{sN+1}^{n-1}). \quad (12)$$

- A sequence of decoder functions $g_r : \mathcal{U} \times \mathcal{Y}_{sN+1}^n \rightarrow \mathcal{W}$, providing an estimate \hat{W}_n of the message W , where $r \in \{1, \dots, N\}$, $n \geq 1$, $s = \lfloor \frac{n-1}{N} \rfloor$:

$$\hat{W}_n = g_r(U, Y_{sN+1}^n). \quad (13)$$

A practical consequence of this definition is that for decision-feedback repeat-after- N codes, only N unique coded symbols need to be generated for each message, due to the fact that $X_n = f_r(U, W)$. Because the decoder in (13) only uses the received symbols from the current

length- N block, we define the following modified information density:

$$i_N(X^n; Y^n) = \log \frac{dP(Y_{sN+1}^n = y_{sN+1}^n | X_{sN+1}^n = x_{sN+1}^n)}{dP(Y_{sN+1}^n = y_{sN+1}^n)} \quad (14)$$

$$= \log \frac{dP(Y^r = y_{sN+1}^n | X^r = x_{sN+1}^n)}{dP(Y^r = y_{sN+1}^n)}. \quad (15)$$

Corollary 1 (Random-coding lower bound for repeat-after- N codes). *Suppose that N is large enough such that $P[\tau \leq N] > 0$. Then for a scalar $\gamma > 0$, \exists an (ℓ, M, ϵ) repeat-after- N VLF code satisfying*

$$\ell \leq E[\tau] = \frac{\sum_{n=0}^{N-1} P[\tau > n]}{1 - P[\tau > N]}, \quad (16)$$

$$\epsilon \leq (M - 1)P[\bar{\tau} \leq \tau], \quad (17)$$

where γ is a threshold for the hitting times τ and $\bar{\tau}$:

$$\tau = \inf\{n \geq 0 : i_N(X^n; Y^n) \geq \gamma\} \quad (18)$$

$$\bar{\tau} = \inf\{n \geq 0 : i_N(\bar{X}^n; Y^n) \geq \gamma\}. \quad (19)$$

We will show in Sec. III that repeat-after- N VLF codes constructed by puncturing convolutional codes can deliver throughput surpassing that of the random-coding lower bound of Thm. 1, even when the random-coding lower bound does not use the repeat-after- N restriction. Similar behavior was seen in Chen et al. [7], [8], which explore the effect of finite-length codewords on the achievable rates of VLFT codes. The proof of Cor. 1 is in Appendix B.

Thm. 1 can also be extended to accommodate repeat-after- N codes that permit decoding only at m specified intervals (modulo N_m): $n \in \{N_1, N_2, \dots, N_m, N_m + N_1, \dots\}$. Similar to the repeat-after- N setting, the coded symbols for $n > N_m$ repeat the first N_m symbols. We define $I_i = N_i - N_{i-1}$ as the transmission length of the i th transmission ($i = 1, \dots, m$), where $N_0 = 0$ for convenience. This framework models practical systems, in which decoding is attempted after groups of symbols instead of after individual symbols. The following corollary provides the achievability result for random coding with “packets” of length I_i .

Corollary 2 (Random-coding lower bound for m -transmission repeat-after- N_m codes). *Suppose that N_m is large enough such that $\mathbb{P}[\tau \leq N_m] > 0$. Then for a scalar $\gamma > 0$, \exists an (ℓ, M, ϵ) m -transmission, repeat-after- N_m VLF code satisfying*

$$\ell \leq \mathbb{E}[\tau] = \frac{\sum_{i=0}^{m-1} I_i \mathbb{P}[\tau > N_i]}{1 - \mathbb{P}[\tau > N_m]}, \quad (20)$$

$$\epsilon \leq (M - 1)\mathbb{P}[\bar{\tau} \leq \tau], \quad (21)$$

where γ is a threshold for the hitting times τ and $\bar{\tau}$:

$$\tau = \inf\{n \geq 0 : i_N(X^n; Y^n) \geq \gamma\} \cap \{N_1, N_2, \dots, N_m, N_m + N_1, \dots\}, \quad (22)$$

$$\bar{\tau} = \inf\{n \geq 0 : i_N(\bar{X}^n; Y^n) \geq \gamma\} \cap \{N_1, N_2, \dots, N_m, N_m + N_1, \dots\}. \quad (23)$$

The proof of Cor. 2 is omitted. It closely follows that of Cor. 1 and relies on the fact that decoding can only occur at the specified intervals, so the expected stopping time in (20) is a sum of probabilities weighted by the i th transmission length I_i .

As shown in Fig. 2(a) for the binary symmetric channel (BSC) with crossover probability $p = 0.05$, there is a considerable gap between the lower and upper bounds on the maximum rate of VLF codes at short blocklengths. Because of this gap in the fundamental limits, it is not clear what finite-blocklength performance is achievable. To explore this question, we present a deterministic coding scheme in Sec. III, fixing M and ϵ to explore what rates can be achieved at short blocklengths (less than 300 symbols).

III. CONVOLUTIONAL CODES WITH DECISION FEEDBACK

A. Reliability-based Error Detection

This section investigates the performance of punctured convolutional codes with decision feedback in the context of Sec. II's VLF coding framework. Many hybrid ARQ systems with convolutional codes use CRCs for explicit error detection at the receiver, sometimes referred to

as code-based retransmission. However, at short blocklengths, the latency overhead of a CRC strong enough to meet the ϵ error constraint may result in a significant rate penalty. Here we investigate the performance of reliability-based retransmission at short blocklengths, in which the receiver stops decoding when the posterior probability of the decoded word is at least $(1 - \epsilon)$. This approach guarantees that the ϵ error requirement is met and does not require additional coded symbols to be sent for error detection.

For practical purposes, we consider only repeat-after- N codes in this section. After receiving the n th transmitted symbol, the receiver computes the posterior probability (the reliability) of the maximum a posteriori (MAP) message \hat{W}_n , where

$$\hat{W}_n = \arg \max_{i \in \mathcal{W}} P(W = i | Y_{sN+1}^n). \quad (24)$$

The stopping rule for the reliability-based (RB) retransmission scheme is defined according to:

$$\tau^{(\text{RB})} = \inf\{n \geq 0 : P(W = \hat{W}_n | Y_{sN+1}^n) \geq 1 - \epsilon\}. \quad (25)$$

Finding the MAP message in (24) may be accomplished by computing all M posterior probabilities in (24), which can in principle be performed for any code, such as LDPC codes. However, even for moderate blocklengths, this may not be computationally feasible, similar to the complexity challenge of ML decoding. Fortunately, for terminated convolutional codes, Raghavan and Baum's ROVA [16] gives an efficient method to compute $P(W = \hat{W}_n | Y_{sN+1}^n)$, the posterior probability of the MAP message¹. The computational complexity of the ROVA is linear in the blocklength and exponential in the constraint length, on the same order as that of the Viterbi Algorithm. This allows the receiver to implement the stopping rule in (25) without explicitly evaluating all M posterior probabilities. Due to this rule, the overall probability of

¹When the source symbols are equiprobable, there is a one-to-one correspondence between the MAP message and the ML codeword, the latter of which is identified by both the Viterbi Algorithm and the ROVA.

error in the reliability-based stopping scheme will satisfy the ϵ constraint:

$$\mathbb{P}[\hat{W}_{\tau^{(\text{RB})}} \neq W] = \mathbb{E}[1 - \mathbb{P}[\hat{W}_{\tau^{(\text{RB})}} = W | Y_{sN+1}^{\tau^{(\text{RB})}}]] \leq \epsilon. \quad (26)$$

An alternative algorithm for computing the MAP message probability for terminated convolutional codes is given by Hof et al. [24], which provides a modification to the Viterbi Algorithm that permits decoding with erasures according to Forney's generalized decoding rule [19]. The MAP message probability can also be computed approximately by Fricke and Hoeher's simplified (approximate) ROVA [25].

However, terminated convolutional codes suffer from rate loss at short blocklengths, as described earlier, and Raghavan and Baum's ROVA [16] does not permit decoding of throughput-efficient tail-biting convolutional codes (TBCCs). Williamson et al. [17]'s tail-biting ROVA describes how to compute the posterior probability of MAP messages corresponding to tail-biting codewords. In the simulations that follow, we use both the ROVA for terminated codes and, when computational complexity permits, the TB ROVA for tail-biting codes. In particular, we implement an efficient version of the TB ROVA called the Tail-Biting State-Estimation Algorithm (TB SEA) from [17] that reduces the number of computations but still computes the MAP message probability exactly².

The details of our decision-feedback scheme are as follows. Similar to Fricke and Hoeher [13]'s reliability-based retransmission criteria for hybrid ARQ, if the computed word-error probability at blocklength n is greater than the target ϵ , the decoder signals that additional coded symbols are required (sends a NACK), and the transmitter sends another coded symbol. When the word-error probability is less than ϵ , the decoder sends an ACK, and transmission stops. We encode a message with $k = \log M$ message symbols into a mother codeword of length N . One symbol is transmitted at a time, using pseudo-random, rate-compatible puncturing of the mother code. At

²The TB SEA and TB ROVA compute the same probability as long as $\mathbb{P}(W = \hat{W}_n | Y) > \frac{1}{2}$. In the proposed reliability-based retransmission scheme with $\epsilon < \frac{1}{2}$, this condition is met for $\tau^{(\text{RB})} = n$, so the TB SEA is an ML sequence decoder.

each decoding opportunity, the receiver uses all received symbols to decode and computes the MAP message probability. If the receiver requests additional redundancy after N symbols have been sent, the transmitter begins resending the original sequence of N symbols and decoding starts from scratch. (This is a repeat-after- N VLF code.) While some benefit can be accrued by retaining the N already-transmitted symbols (for example, by Chase code combining), we do not exploit this opportunity in our scheme for the sake of simplicity.

Similar to the random-coding lower bound for repeat-after- N codes in Cor. 1, we can express the latency $\lambda^{(\text{RB})}$ and the throughput $R_t^{(\text{RB})}$ of the proposed scheme as

$$\lambda^{(\text{RB})} \leq \frac{1 + \sum_{i=1}^{N-1} P_{\text{NACK}}(i)}{1 - P_{\text{NACK}}(N)}, \quad (27)$$

$$R_t^{(\text{RB})} = \frac{k}{\lambda^{(\text{RB})}} (1 - P_{\text{UE}}), \quad (28)$$

where $P_{\text{NACK}}(i)$ is the probability that a NACK is generated because the MAP message probability is less than $(1 - \epsilon)$ when i coded symbols (modulo N) have been received, and P_{UE} is the overall probability of undetected error. Note $P_{\text{UE}} \leq \epsilon$ by definition of the stopping rule, as shown in (26). We obtain $P_{\text{NACK}}(i)$ and P_{UE} via simulation in the following section and plot the resulting $(\lambda^{(\text{RB})}, R_t^{(\text{RB})})$ pairs. We have included the factor $(1 - P_{\text{UE}})$ in the throughput expression to emphasize that we are only counting the messages that are decoded both correctly and with sufficient reliability at the receiver (i.e., the goodput).

B. Convolutional Code Polynomials

This section briefly lists the convolutional code polynomials used in the subsequent VLF coding simulations. We use both terminated convolutional codes and tail-biting convolutional codes for the ROVA-based stopping rule. Comparisons with CRCs use only tail-biting convolutional codes.

Table I, taken from Lin and Costello [26, Table 12.1], lists the generator polynomials for the rate-1/3 convolutional codes that were used as the mother codes for our simulations. Each code

TABLE I

GENERATOR POLYNOMIALS g_1 , g_2 , AND g_3 CORRESPONDING TO THE RATE 1/3 CONVOLUTIONAL CODES USED IN THE VLF SIMULATIONS. d_{FREE} IS THE FREE DISTANCE, $A_{d_{\text{FREE}}}$ IS THE NUMBER OF CODEWORDS WITH WEIGHT d_{FREE} , AND L_D IS THE ANALYTIC TRACEBACK DEPTH.

# Memory Elements, ν	# States $s = 2^\nu$	Polynomial (g_1, g_2, g_3)	d_{free}	$A_{d_{\text{free}}}$	L_D
6	64	(117, 127, 155)	15	3	21
8	256	(575, 623, 727)	18	1	25
10	1024	(2325, 2731, 3747)	22	7	34

selected has the optimum free distance d_{free} , which is listed along with the analytic traceback depth L_D [27]. Higher-rate codewords used for the incremental transmissions are created by pseudorandom, rate-compatible puncturing of the rate-1/3 mother codes.

All of the simulations involving the AWGN channel use the binary-input AWGN channel (i.e., using BPSK signaling) with soft-decision decoding. The binary-input AWGN channel has a maximum Shannon capacity of 1 bit per channel use, even when the SNR η is unbounded. However, we have included comparisons with the capacity of the full AWGN channel (i.e., with real-valued inputs drawn i.i.d. $\sim \mathcal{N}(0, \eta)$). For the SNRs and capacities used in our examples, the binary-input restriction is a minor concern.

C. Numerical Results

Fig. 2(a) illustrates the short-blocklength performance of the reliability-based retransmission scheme using the ROVA for terminated convolutional codes, compared to the fundamental limits for VLF codes. This example uses the BSC with crossover probability $p=0.05$ and target probability of error $\epsilon=10^{-3}$. The Shannon (asymptotic) capacity of the BSC with crossover probability p is $C_{\text{BSC}} = 1 - h_b(p)$. The random-coding lower bound (‘VLF achievability’) is from Thm. 1 and the upper bound (‘VLF converse’) is from [6, Theorem 6]. An example of

the random-coding lower bound for repeat-after- N codes from Cor. 1 is also shown (‘VLF achievability, repeat-after- N ’), with $N = 3 \log M$, which corresponds to our implementations with a rate-1/3 mother code. Both the convolutional code simulations and the VLF bounds correspond to decoding after every received symbol. Fig. 2(a) also includes the maximum rate at finite blocklengths without feedback (‘Fixed-length code, no feedback’), based on the normal approximation from [5].

Though the upper and lower bounds for VLF codes coincide asymptotically, there is a considerable gap when latency is below 100 bits, a region in which convolutional codes can deliver good performance. At the shortest blocklengths, the 64-state code with fewer memory elements performs best, due to the rate loss of the codes with larger constraint lengths. However, as the message length k increases (and the latency increases), the more powerful 1024-state code delivers superior throughput. As the latency continues to increase, the codes’ throughputs fall below that of the VLF achievability bound, which is based on random coding. Random coding improves with latency, but the word-error probability of convolutional codes increases with blocklength once the blocklength is beyond twice the traceback depth L_D of the convolutional code [27]. Note the $(\lambda^{(\text{RB})}, R_t^{(\text{RB})})$ curve for the 64-state code exhibits non-monotonic behavior near $\lambda^{(\text{RB})}=17$ ($k=8$), likely due to non-monotonic minimum distance growth of the terminated convolutional codes as a function of blocklength, in conjunction with non-ideal effects of pseudo-random puncturing. The maximum throughput obtained for these BSC simulations is $R_t^{(\text{RB})} = 0.551$ bits per channel use at $\lambda^{(\text{RB})} = 147.06$ bits for the $k = 91$, 1024-state code, which is 77.2% of the BSC capacity.

Fig. 2(b) shows the performance of the reliability-based retransmission scheme over the AWGN channel with SNR 2 dB and target $\epsilon=10^{-3}$. The Shannon capacity of the AWGN channel with SNR η is $C_{\text{AWGN}} = \frac{1}{2} \log(1 + \eta)$, and the Shannon capacity of the BI-AWGN channel is approximated as in [28]. The random-coding lower bound (‘VLF achievability’) is from Thm. 1, the AWGN upper bound (‘VLF converse, AWGN’) is from [6, Theorem 4] and particularized

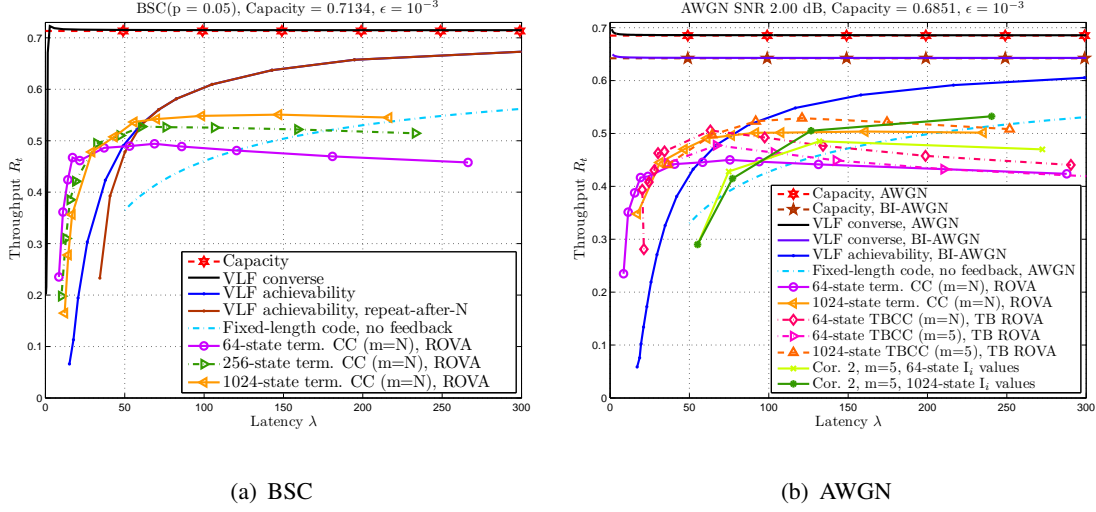


Fig. 2. Short-blocklength performance of the reliability-based retransmission scheme with target probability of error $\epsilon = 10^{-3}$. Simulations use the ROVA for terminated convolutional codes (term. CC) and the TB ROVA for tail-biting convolutional codes (TBCC), with decoding after every symbol ($m=N$) or with decoding after $m=5$ groups of symbols. Simulations are over (a) the BSC($p = 0.05$) or (b) over the AWGN channel with SNR 2.00 dB.

to the Gaussian channel, and the BI-AWGN upper bound (‘VLF converse, BI-AWGN’) is from [6, Theorem 6]. The “Fixed-length code, no feedback” curve uses the normal approximation [5]. The terminated convolutional code (term. CC) simulations in Fig. 2(b) use the ROVA and attempt decoding after every symbol, as in Fig. 2(a). Similar performance is observed as in the BSC case. The throughput of the convolutional codes surpasses the random-coding lower bound at short blocklengths, but plateaus around latencies of 100 bits. Convolutional codes with more memory elements would be expected to deliver improved throughput, but computational complexity limits us to codes with 1024 states or fewer. Additionally, the high decoding complexity of the 1024-state codes prevented us from decoding after every symbol when using the TB ROVA.

D. Decoding after Groups of Symbols

Decoding less frequently is practically desirable due to the round-trip delay inherent in the feedback loop and because of the complexity associated with performing the ROVA after each

received symbol. Decoding with the ROVA only after packets is a natural extension of the proposed scheme, akin to the m -transmission repeat-after- N_m codes in Sec. II. When decoding only after packets are received, the latency $\lambda^{(\text{RB})}$ and the throughput $R_t^{(\text{RB})}$ become

$$\lambda^{(\text{RB})} \leq \frac{I_1 + \sum_{i=1}^{m-1} I_i P_{\text{NACK}}(N_i)}{1 - P_{\text{NACK}}(N_m)}, \quad (29)$$

$$R_t^{(\text{RB})} = \frac{k}{\lambda^{(\text{RB})}} (1 - P_{\text{UE}}). \quad (30)$$

Here $P_{\text{NACK}}(N_i)$ is the probability of retransmission when N_i coded symbols have been received. The incremental transmission length at transmission i is I_i and the cumulative decoding blocklength is $N_i = I_1 + \dots + I_i$.

A main challenge in an m -transmission incremental redundancy scheme is to select the set of m incremental transmission lengths $\{I_i\}_{i=1}^m$ that provide the best rate at short blocklengths. In general, latency (resp., throughput) expressions such as (29) (resp., (30)) are not convex (resp., concave) in the blocklengths and must be optimized numerically. Appendix C presents an algorithm to optimize the blocklengths in general incremental redundancy schemes. Appendix D describes how to particularize the algorithm in order to select the $m=5$ optimal blocklengths in the reliability-based retransmission scheme using the TB ROVA for TBCCs.

Table II shows the optimal transmission lengths identified by the blocklength-selection algorithm. Based on these blocklengths, we simulated the TB ROVA with TBCCs in an $m=5$ transmission decision-feedback scheme. Fig. 2(b) shows the impact on throughput when decoding is limited to these specified decoding opportunities. Despite fewer opportunities for decoding (and hence fewer chances to stop transmission early), both the 64-state and 1024-state tail-biting codes in the optimized $m=5$ setting deliver excellent performance compared to the respective terminated codes that allow decoding after every symbol (i.e., $m=N$). Note also how at blocklengths less than approximately 75 bits, the $m=5$ TBCCs deliver higher rates than the random-coding lower bound that requires decoding after every symbol ('VLF' achievability,

TABLE II

OPTIMAL TRANSMISSION LENGTHS $\{I_i\}^*$ FOR THE $m=5$ TRANSMISSION SCHEME USING THE TB ROVA, FOR SNR $\eta=2$ DB, ALONG WITH THE SIMULATED ERROR PROBABILITY P_{UE} CORRESPONDING TO TARGET ERROR PROBABILITY $\epsilon=10^{-3}$.

Info. Bits k	Target Error ϵ	64-state TBCC		1024-state TBCC	
		Transmission Lengths $\{I_1^*, I_2^*, I_3^*, I_4^*, I_5^*\}$	Simulated Error P_{UE}	Transmission Lengths $\{I_1^*, I_2^*, I_3^*, I_4^*, I_5^*\}$	Simulated Error P_{UE}
16	10^{-3}	30, 3, 3, 5, 7	2.260×10^{-4}	29, 4, 4, 4, 7	2.473×10^{-4}
32	10^{-3}	57, 6, 7, 9, 16	1.960×10^{-4}	56, 5, 5, 7, 12	1.976×10^{-4}
48	10^{-3}	88, 9, 10, 13, 24	2.350×10^{-4}	80, 7, 7, 9, 16	2.085×10^{-4}
64	10^{-3}	121, 12, 13, 17, 29	2.600×10^{-4}	106, 9, 9, 12, 22	1.993×10^{-4}
91	10^{-3}	178, 17, 18, 22, 38	2.650×10^{-4}	151, 13, 14, 17, 31	2.197×10^{-4}
128	10^{-3}	261, 23, 24, 30, 46	2.440×10^{-4}	223, 17, 18, 24, 44	2.344×10^{-4}

BI-AWGN'). When compared to Cor. 2's random-coding lower bound for repeat-after- N_m codes on the AWGN channel ('Repeat-after-N ($m=5$)'), the $m=5$ TBCCs deliver higher rates for blocklengths up to about 125 bits. The 'Cor. 2, $m=5$, 64-state I_i values' curve uses the optimal $m=5$ blocklengths for the 64-state TBCC, and the 1024-state curve uses the optimal $m=5$ blocklengths for the 1024-state TBCC. The maximum throughput obtained from these $m=5$ simulations is $R_t^{(\text{RB})} = 0.529$ bits per channel use at $\lambda^{(\text{RB})} = 121.0$ bits, for the $k=64$, 1024-state code. This is 77.2% of the AWGN capacity and 82.4% of the BI-AWGN capacity.

For all of the VLF simulations in this section, at least 25 undetected word-errors were accumulated for each value of k . Because the ROVA-based stopping rule with target $\epsilon=10^{-3}$ guarantees that the average probability of error is no more than 10^{-3} , it is not important for us to characterize the empirical error probability exactly. For this paper, we are more concerned with the performance in terms of throughput and latency. Observations from VLF simulations show that collecting at least 25 word errors is sufficient for estimating the throughput and latency.

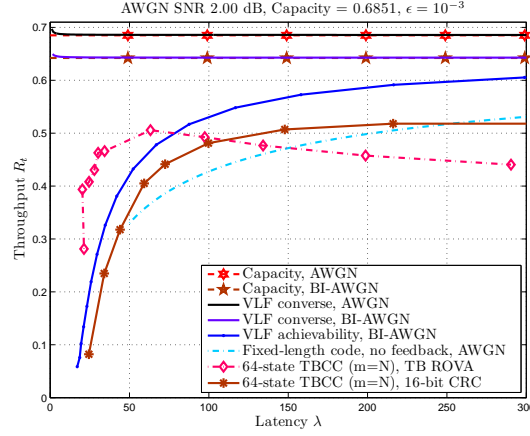


Fig. 3. A comparison of two decision-feedback schemes, the reliability-based retransmission scheme with the TB ROVA and the code-based approach with 16-bit CRCs. Using the TB ROVA guarantees the probability of error to be less than ϵ , but CRCs provide no such guarantee. In this example, 16 CRC bits were sufficient to meet the target of $\epsilon=10^{-3}$.

E. Code-based Error Detection

In practice, decision-feedback schemes often use a checksum (e.g., a CRC) at the receiver to detect errors in the decoded word. However, the additional parity bits of a CRC that must be sent impose a latency cost that may be severe at short blocklengths. For an A -bit CRC appended to k message bits, the throughput (not counting the check bits) is $R_t^{(\text{CRC})} = \frac{k}{k+A} R_t$, where R_t is defined similarly to (28) for the reliability-based scheme. Equivalently, the rate-loss factor from an A -bit CRC is $\frac{A}{k+A}$. Using an error-detection code to determine retransmission requests is sometimes referred to as code-based error detection [13], in contrast to reliability-based error detection with the ROVA. As noted in Frick and Hoeher's [13] investigation of reliability-based hybrid ARQ schemes, the rate loss and undetected error probability of the code-based approach depend critically on the blocklengths and target error probabilities involved.

Fig. 3 provides an example of the throughput obtained when decoding after every symbol and using a 16-bit CRC for error detection. After decoding the 64-state TBCC (which has $k+A$ input bits), the receiver re-computes the CRC to check for errors. As expected, the rate loss of the CRCs at blocklengths less than 50 bits severely limits the achievable rates. The 64-state TBCCs

TABLE III

SIMULATED ERROR PROBABILITIES P_{UE} OF THE 16-BIT CRC SIMULATIONS IN FIG. 3 FOR THE 2 dB AWGN CHANNEL. THE 12-BIT CRCs FAIL TO MEET THE ERROR CONSTRAINT OF $\epsilon=10^{-3}$, BUT THE STRONGER 16-BIT CRCs GENERALLY SATISFY THE CONSTRAINT. GENERATOR POLYNOMIALS FOR “GOOD” A -BIT CRCs FROM [29] ARE LISTED IN HEXADECIMAL (E.G., 0XCD INDICATES THE POLYNOMIAL IS $x^8 + x^7 + x^4 + x^3 + x + 1$). THE $k + A$ COLUMN INDICATES THE NUMBER OF INPUT BITS TO THE RATE-1/3 CONVOLUTIONAL ENCODER. CELLS LABELED — INDICATE THAT NO SIMULATIONS WERE RUN FOR THAT VALUE OF $k + A$.

Input Bits $k + A$	P_{UE} 12-bit CRC (0xc07)	P_{UE} 16-bit CRC (0x8810)
24	1.479×10^{-1}	1.000×10^{-4}
30	—	8.618×10^{-4}
34	1.036×10^{-3}	1.077×10^{-3}
40	—	2.105×10^{-4}
48	2.935×10^{-3}	2.025×10^{-4}
64	3.504×10^{-3}	2.538×10^{-4}
91	4.646×10^{-3}	3.017×10^{-4}
128	6.755×10^{-3}	5.370×10^{-4}
181	8.864×10^{-3}	6.667×10^{-4}

decoded with the TB ROVA deliver higher rates until the average blocklength reaches about 75 to 100 bits. For moderately large blocklengths (e.g., 150 bits and greater), the throughput penalty induced by CRCs becomes less severe. (As the information length k increases, the rate-loss factor $\frac{A}{k+A}$ decays to zero.) Note that decoding after every symbol prevents simulation of higher-constraint-length convolutional codes (e.g., 1024-state codes).

Importantly, using ROVA guarantees the probability of error to be less than ϵ (as long as the length- N mother code is long enough to meet this constraint on average), but CRCs provide no such guarantee. In this example, in fact, TBCC simulations with 12-bit CRCs failed to meet the target of $\epsilon=10^{-3}$, as shown in Table III. As a result, the codes with 12-bit CRCs do not qualify as $(\ell, M=2^k, \epsilon=10^{-3})$ VLF codes, so the VLF codes with 12-bit CRCs is not plotted in Fig. 3. Both the 12-bit and 16-bit CRC polynomials are from [29] and are listed in Table III.

The 16-bit CRCs in this example generally provide sufficiently low error probabilities, but at the expense of reduced rate versus the 12-bit CRCs. One exception when the 16-bit CRC fails to meet the $\epsilon=10^{-3}$ constraint in our simulations is when $k + A = 34$ ($k \approx A = 16$), as shown in Table III. This high error probability seems to be an outlier compared to the other 16-bit CRC simulations, but is consistent with findings from previous CRC research, such as [30]. In [30], Witzke and Leung show that the undetected error probability of a given A -bit CRC polynomial over the BSC can vary widely as a function of the channel bit-error rate, especially for small values of k . The present variable-length simulations complicate matters further, due to the stopping rule that terminates when the CRC matches, even if erroneously. Additional simulations with $k + A = 30$ and $k + A = 40$ were performed in order to illustrate the sensitivity of the error probability to the information length k (Table III).

In general, it is difficult to determine exactly how many CRC bits should be used to provide the maximum throughput for hybrid ARQ schemes, since the error probability depends on the SNR. Communication system designers will likely be tempted to conservatively select large CRC lengths, which restricts the short-blocklength throughput. In contrast, the ROVA-based approach always guarantees a maximum error probability. Still, future work that explores the performance of VLF codes at larger blocklengths (e.g., 400 bits and above) may benefit from code-based error detection.

IV. CONCLUSION

This paper demonstrated a reliability-based decision-feedback scheme that provides throughput surpassing the random-coding lower bound at short blocklengths. We selected convolutional codes for their excellent performance at short blocklengths and used the tail-biting ROVA to avoid the rate loss of terminated convolutional codes. For both the BSC and AWGN channels, convolutional codes provided throughput above 77% of capacity, with blocklengths less than 150 bits. While codes with higher constraint lengths would be expected to provide superior perfor-

mance, computational considerations limited us to evaluate 64-state codes with the TB ROVA and decoding after every symbol, and 1024-state codes with the TB ROVA in an $m=5$ transmission incremental redundancy setting. We introduced a novel blocklength-selection algorithm to aid in selecting the $m=5$ transmission lengths and showed that despite the limitations on decoding frequency, the incremental redundancy scheme is competitive with decoding after every symbol. Finally, we demonstrated that the latency overhead of CRCs imposes a severe rate-loss penalty at short blocklengths, whereas reliability-based decoding does not require transmission of separate error-detection bits.

APPENDIX

A. Numerical Computation of the VLF Lower Bound

For channels with bounded information density, Wald's equality (also known as Wald's identity or Wald's lemma) allows us to compute an upper bound on the expected stopping time $E[\tau]$ in the random-coding lower bound of Thm. 1 as follows:

$$E[\tau] \leq \frac{\log(M-1) + \log \frac{1}{\epsilon} + B}{C}, \quad (31)$$

where $B < \infty$ is the upper bound on the information density: $B = \sup_{x \in \mathcal{X}, y \in \mathcal{Y}} i(x; y)$.

Proof: Defining $S_j = i(X_j; Y_j) = \log \frac{P(Y_j|X_j)}{P(Y_j)}$, we have

$$S^n = i(X^n; Y^n) = \log \frac{P(Y^n|X^n)}{P(Y^n)} \quad (32)$$

$$= \sum_{j=1}^n \log \frac{P(Y_j|X_j)}{P(Y_j)} \quad (33)$$

$$= \sum_{j=1}^n S_j, \quad (34)$$

where (33) follows due to the random codebook generation. Since the S_j are i.i.d with $E[S_j] = C$, Wald's equality gives the following result [23, Ch. 5] :

$$E[S^\tau] = E[\tau]E[S_1]. \quad (35)$$

This leads to the following upper bound on $E[\tau]$:

$$E[\tau] = \frac{E[S^\tau]}{C} \quad (36)$$

$$= \frac{E[S^{\tau-1} + S_\tau]}{C} \quad (37)$$

$$\leq \frac{\gamma + B}{C}, \quad (38)$$

where (38) follows from the definition of the threshold γ in Thm. 1 and of B above.

Recall that the error probability ϵ is upper bounded in Thm. 1 as $\epsilon \leq (M-1)P[\bar{\tau} \leq \tau]$. This can be further upper bounded as follows, as in [6] and [15, Appendix B]:

$$P[\bar{\tau} \leq n] = E[1\{\bar{\tau} \leq n\}] \quad (39)$$

$$= E[1\{\tau \leq n\} \exp\{-i(X^\tau; Y^\tau)\}] \quad (40)$$

$$\leq \exp\{-\gamma\}, \quad (41)$$

because $i(X^\tau; Y^\tau) \geq \gamma$ by definition. Thus, we can write

$$P[\bar{\tau} \leq \tau] = \sum_{n=0}^{\infty} P[\tau = n]P[\bar{\tau} \leq n] \quad (42)$$

$$\leq \sum_{n=0}^{\infty} P[\tau = n] \exp\{-\gamma\} \quad (43)$$

$$\leq \exp\{-\gamma\}. \quad (44)$$

Therefore, the bound on error probability can be loosened to $\epsilon \leq (M-1) \exp\{-\gamma\}$. Rearranging gives $\gamma \leq \log \frac{M-1}{\epsilon}$ and, when combined with (38), yields the following:

$$E[\tau] \leq \frac{\log \frac{M-1}{\epsilon} + B}{C}, \quad (45)$$

which proves (31). ■

Examples: For the BSC(p), $B = \log 2(1-p)$. For the BI-AWGN channel, $B = \log 2$ (regardless of the SNR). ■

B. Proof of Cor. 1 (Random-coding lower bound for repeat-after- N codes)

Proof: The proof closely follows that of [6, Theorem 3]. We define M stopping times τ_j , $j \in \{1, \dots, M\}$, one for each codeword:

$$\tau_j = \inf\{n \geq 0 : i_N(X^n(j); Y^n) \geq \gamma\}, \quad (46)$$

where $X^n(j)$ is the first n symbols of the j th codeword. At each n , the decoder evaluates the M information densities $i_N(X^n(j); Y^n)$ and makes a final decision at time τ^* when the first of these (possibly more than one at once) reaches the threshold γ :

$$\tau^* = \min_{j=1, \dots, M} \tau_j. \quad (47)$$

The decoder at time τ^* selects codeword $m = \max\{j : \tau_j = \tau^*\}$. The average blocklength $\ell = \mathbb{E}[\tau^*]$ is upper bounded as follows:

$$\mathbb{E}[\tau^*] \leq \frac{1}{M} \sum_{j=1}^M \mathbb{E}[\tau_j | W = j] \quad (48)$$

$$= \mathbb{E}[\tau_1 | W = 1] \quad (49)$$

$$= \mathbb{E}[\tau] \quad (50)$$

$$= \sum_{n=0}^{\infty} \mathbb{P}[\tau > n] \quad (51)$$

$$= (1 + \mathbb{P}[\tau > N] + \mathbb{P}[\tau > N]^2 + \dots) \sum_{n=0}^{N-1} \mathbb{P}[\tau > n] \quad (52)$$

$$= \frac{\sum_{n=0}^{N-1} \mathbb{P}[\tau > n]}{1 - \mathbb{P}[\tau > N]}. \quad (53)$$

Eq. (49) follows from the symmetry of the M stopping times and (50) is by the definition of τ as given in (18). Because the modified information densities depend only on the symbols in the current N -block, repeat-after- N VLF codes satisfy the following property, which leads to (52):

$$\mathbb{P}[\tau > n] = \mathbb{P}[\tau > N]^s \mathbb{P}[\tau > r], \quad (54)$$

where $n = sN + r$. The condition that $P[\tau \leq N] > 0$ in Cor. 1 is required so that $P[\tau > N] < 1$, guaranteeing that the sum in (52) will converge.

Using \hat{W}_n to denote the decoder's decision at time n , an error occurs if the decoder chooses $\hat{W}_{\tau^*} \neq W$. The probability of error ϵ can be bounded due to the random codebook generation:

$$\epsilon = P[\hat{W}_{\tau^*} \neq W] \quad (55)$$

$$\leq P[\hat{W}_{\tau^*} \neq 1 | W = 1] \quad (56)$$

$$\leq P[\tau_1 \geq \tau^* | W = 1] \quad (57)$$

$$\leq P\left[\bigcup_{j=2}^M \{\tau_1 \geq \tau_j\} | W = 1\right] \quad (58)$$

$$\leq (M - 1)P[\tau_1 \geq \tau_2 | W = 1] \quad (59)$$

$$= (M - 1)P[\tau \geq \bar{\tau}]. \quad (60)$$

The last line follows because $(\tau, \bar{\tau})$ have the same distribution as (τ_1, τ_2) conditioned on $W = 1$. ■

C. General Blocklength-selection Algorithm

Selecting the m incremental transmission lengths $\{I_i\}^*$ that minimize the latency (or equivalently, maximize the throughput) of VLF coding schemes is non-trivial. The complexity of a brute-force search grows exponentially with m . In this section, we describe an efficient blocklength-selection algorithm that can be used to identify suitable blocklengths for general incremental redundancy schemes. The goal of the algorithm is to select the m integer-valued incremental transmission lengths $\{I_i\}^*$ as follows:

$$\{I_i\}^* = \arg \min_{\{I_i\} \in \mathbb{Z}} \lambda \quad \text{s.t.} \quad P_{\text{UE}} \leq \epsilon. \quad (61)$$

For the decision-feedback scheme using the TB ROVA in Sec. III, the probability of undetected error is less than ϵ by definition, so the constraint can be ignored.

The proposed blocklength-selection algorithm for an m -transmission incremental redundancy scheme follows. Starting from a pseudo-random initial vector $\{I_1, I_2, \dots, I_m\}$, the algorithm performs coordinate descent, wherein one transmission length I_i is optimized while all others are held fixed. The objective function λ is evaluated for positive and negative unit steps in increment I_i , i.e., for the transmission length vectors $\{I_1, \dots, I_i + 1, \dots, I_m\}$ and $\{I_1, \dots, I_i - 1, \dots, I_m\}$. Length I_i is updated if the objective improves. Once the objective cannot be improved by any single-coordinate steps, diagonal steps from each of the possible two-coordinate pairs (I_i, I_j) are evaluated. For each two-coordinate pair, four possible neighboring diagonal steps are evaluated. The transmission lengths I_i and I_j are updated if the best of the four diagonal steps improves the objective λ . This continues until the objective cannot be improved by additional diagonal steps. The entire process then starts over from another pseudo-random initial vector. Random restarts are employed in order to avoid getting stuck at local optima of λ , of which there can be many. Empirical trials of this algorithm for several different families of retransmission probabilities demonstrated significantly reduced computation time compared to a brute-force approach (which is in general not possible for large k). Furthermore, while this algorithm is not guaranteed to find the global optimum, results show that the final objective value λ_{best} was improved compared to results from an earlier quasi-brute-force trial.

D. TB ROVA Version of Blocklength-selection Algorithm

For the decision-feedback scheme of Sec. III that uses the TB ROVA to compute the posterior probability of the decoded word, the probability of retransmission $P_{\text{re}}(N)$ is the probability that

the posterior at blocklength N is less than $(1 - \epsilon)$, which is difficult to determine analytically.³ Instead, we obtained estimates of the empirical retransmission-probabilities of the rate-1/3 convolutional codes in Table I and used those estimates of $P_{\text{re}}(N)$ to compute the objective λ in the algorithm. To do so, we first simulated fixed-length transmission of rate-1/3, tail-biting convolutional codes from Table I at a small number of pseudo-randomly punctured blocklengths N_{sim} for each fixed message-size k , where $N_{\text{sim}} \in \{k, k + \frac{k}{4}, k + \frac{2k}{4}, \dots, k + \frac{11k}{4}, 3k\}$. For each (k, N_{sim}) pair, we counted the number of decoded words with posterior probability less than $(1 - \epsilon)$, indicating that a retransmission would be required, until there were at least 100 codewords that would trigger a retransmission. We computed $P_{\text{re}}(N_{\text{sim}})$ according to

$$P_{\text{re}}(N_{\text{sim}}) = \frac{\# \text{ codewords triggering retransmission}}{\text{total \# codewords simulated}}. \quad (62)$$

The full set of estimated retransmission probabilities $\tilde{P}_{\text{re}}(N)$ for $N \in \{1, \dots, 3k\}$ was then obtained by a log-polynomial interpolation of the simulated values of $P_{\text{re}}(N_{\text{sim}})$. Finally, the estimated probabilities were used in the algorithm from Appendix C to select the optimal transmission lengths $\{I_i\}^*$. We used 100 random restarts in our implementation. The performance of the TB ROVA-based retransmission scheme using these $m=5$ optimal blocklengths is evaluated in Sec. III.

REFERENCES

- [1] C. E. Shannon, "The zero error capacity of a noisy channel," *IRE Trans. Inf. Theory*, vol. 2, no. 3, pp. 8–19, Sep. 1956.
- [2] D. Mandelbaum, "An adaptive-feedback coding scheme using incremental redundancy (corresp.)," *IEEE Trans. Inf. Theory*, vol. 20, no. 3, pp. 388 – 389, May 1974.

³For a given convolutional code, the weight spectrum for each blocklength N could be used to bound or approximate the posterior probability and that could be used to bound or approximate the retransmission probability, but spectrum-based approaches tend not to be tight over a wide range of SNRs. Further complicating the task is the weight spectrum must be based on a rate-compatible puncturing pattern. Instead of optimizing this puncturing pattern, we use the same pseudo-random puncturing pattern throughout.

- [3] J. Hagenauer, “Rate-compatible punctured convolutional codes (RCPC codes) and their applications,” *IEEE Trans. Commun.*, vol. 36, no. 4, pp. 389–400, Apr. 1988.
- [4] M. V. Burnashev, “Data transmission over a discrete channel with feedback. Random transmission time,” *Probl. Inf. Transm.*, vol. 12, no. 4, pp. 10–30, 1976.
- [5] Y. Polyanskiy, H. V. Poor, and S. Verdú, “Channel coding rate in the finite blocklength regime,” *IEEE Trans. Inf. Theory*, vol. 56, no. 5, pp. 2307–2359, May 2010.
- [6] —, “Feedback in the non-asymptotic regime,” *IEEE Trans. Inf. Theory*, vol. 57, no. 8, pp. 4903–4925, Aug. 2011.
- [7] T.-Y. Chen, A. R. Williamson, and R. D. Wesel, “Variable-length coding with feedback: Finite-length codewords and periodic decoding,” in *Proc. 2013 IEEE Int. Symp. Inf. Theory (ISIT)*, Istanbul, Turkey, July 2013.
- [8] T.-Y. Chen, A. R. Williamson, N. Seshadri, and R. D. Wesel, “Feedback communication systems with limitations on incremental redundancy,” submitted for publication. Available: <http://arxiv.org/abs/1309.0707>.
- [9] T.-Y. Chen, N. Seshadri, and R. D. Wesel, “A sphere-packing analysis of incremental redundancy with feedback,” in *Proc. 2011 IEEE Int. Conf. Commun. (ICC)*, Kyoto, Japan, June 2011.
- [10] —, “Incremental redundancy: A comparison of a sphere-packing analysis and convolutional codes,” in *2011 Inf. Theory and Applications Workshop (ITA)*, San Diego, CA, USA, Feb. 2011.
- [11] E. Visotsky, Y. Sun, V. Tripathi, M. Honig, and R. Peterson, “Reliability-based incremental redundancy with convolutional codes,” *IEEE Trans. Commun.*, vol. 53, no. 6, pp. 987–997, June 2005.
- [12] C. Lott, O. Milenkovic, and E. Soljanin, “Hybrid ARQ: Theory, state of the art and future directions,” in *2007 IEEE Inf. Theory Workshop for Wireless Networks*, Bergen, Norway, July 2007.
- [13] J. Fricke and P. Hoeher, “Reliability-based retransmission criteria for hybrid ARQ,” *IEEE Trans. Commun.*, vol. 57, no. 8, pp. 2181–2184, Aug. 2009.
- [14] A. R. Williamson, T.-Y. Chen, and R. D. Wesel, “Firing the genie: Two-phase short-blocklength convolutional coding with feedback,” in *2013 Inf. Theory and Applications Workshop (ITA)*, San Diego, CA, USA, Feb. 2013.
- [15] —, “Reliability-based error detection for feedback communication with low latency,” in *Proc. 2013 IEEE Int. Symp. Inf. Theory (ISIT)*, Istanbul, Turkey, July 2013.
- [16] A. Raghavan and C. Baum, “A reliability output Viterbi algorithm with applications to hybrid ARQ,” *IEEE Trans. Inf. Theory*, vol. 44, no. 3, pp. 1214–1216, May 1998.
- [17] A. R. Williamson, M. J. Marshall, and R. D. Wesel, “Reliability-output decoding of tail-biting convolutional codes,” *IEEE Trans. Commun.*, vol. 62, no. 6, pp. 1768–1778, June 2014.
- [18] S. Chang, “Theory of information feedback systems,” *IRE Trans. Inf. Theory*, vol. 2, no. 3, pp. 29–40, Sep. 1956.
- [19] G. Forney, “Exponential error bounds for erasure, list, and decision feedback schemes,” *IEEE Trans. Inf. Theory*, vol. 14, no. 2, pp. 206–220, Mar. 1968.
- [20] J. L. Massey, “Causality, feedback and directed information,” in *Proc. 1990 IEEE Int. Symp. Inf. Theory and its Applicat. (ISITA)*, Honolulu, Hawaii, USA, Nov. 1990.

- [21] M. Naghshvar, M. Wigger, and T. Javidi, “Optimal reliability over a class of binary-input channels with feedback,” in *Proc. 2012 IEEE Inf. Theory Workshop (ITW)*, Sep. 2012, pp. 391–395.
- [22] M. Naghshvar, T. Javidi, and M. A. Wigger, “Extrinsic Jensen-Shannon divergence: Applications to variable-length coding,” submitted for publication. Available: <http://arxiv.org/abs/1307.0067>.
- [23] R. G. Gallager, *Stochastic Processes: Theory for Applications*. Cambridge, UK: Cambridge Univ. Press, 2013.
- [24] E. Hof, I. Sason, and S. Shamai (Shitz), “On optimal erasure and list decoding schemes of convolutional codes,” in *Proc. Tenth Int. Symp. Commun. Theory and Applications (ISCTA)*, July 2009, pp. 6–10.
- [25] J. Fricke and P. Hoeher, “Word error probability estimation by means of a modified Viterbi decoder,” in *Proc. 66th IEEE Veh. Technol. Conf. (VTC)*, Oct. 2007, pp. 1113–1116.
- [26] S. Lin and D. J. Costello, *Error Control Coding, Second Edition*. Upper Saddle River, NJ, USA: Prentice-Hall, Inc., 2004.
- [27] J. Anderson and K. Balachandran, “Decision depths of convolutional codes,” *IEEE Trans. Inf. Theory*, vol. 35, no. 2, pp. 455–459, Mar. 1989.
- [28] A. O. Nasif and G. N. Karystinos, “Binary transmissions over additive Gaussian noise: A closed-form expression for the channel capacity,” in *Proc. 2005 Conf. Inf. Sci. and Syst. (CISS)*, Baltimore, MD, USA, Mar. 2005.
- [29] P. Koopman and T. Chakravarty, “Cyclic redundancy code (CRC) polynomial selection for embedded networks,” in *2004 IEEE Int. Conf. Dependable Systems and Networks (DSN)*, July 2004, pp. 145 – 154.
- [30] K. Witzke and C. Leung, “A comparison of some error detecting CRC code standards,” *IEEE Trans. Commun.*, vol. 33, no. 9, pp. 996–998, Sep. 1985.